

Towards Automating the Selection of Ground Control Points in Radarsat Images Using a Topographic Database and Vector-Based Data Matching

I. Couloigner, K.P.B. Thomson, Y. Bédard, B. Moulin, E. LeBlanc, C. Djima, C. Latouche, and N. Spicher

Abstract

Users of Radarsat images need ground control points (GCPs) to georeference their images, to rectify them, and to fuse these images. Because the selection of GCPs is usually done manually, the efficiency of the process depends on the ability of the operator to select a GCP. The present paper introduces a new method to automatically identify GCPs in Radarsat images using a topographic database. First, different strategies are elaborated to fit different contexts (topography, cost, availability of data, etc.). These strategies are then grouped in two approaches, i.e., vector-based data matching and raster-based data matching. Both approaches rely on matching feature classes (in ISO/TC211 parlance), e.g., matching "water bodies" or matching "roads intersections" from the image with their equivalent on the topographic database. A user of this method can easily follow the various steps of the GCPs selection process with the support of software tools. This paper presents in detail the method developed to select GCPs with the feature class "water body" and the vector-based matching approach, and also presents some applications.

Introduction

Most Radarsat applications require images that are geometrically corrected. It is quite usual that Radarsat images are integrated into geographic information systems (GISs) containing multi-source data. Furthermore, as the main advantage of synthetic aperture radar (SAR) images is the reliability of data acquisition even through cloud cover, it is often useful to integrate a set of Radarsat images from various dates for a given area. Radarsat images can also be fused with optical images to obtain complementary information in a single image. Such a comparison of multi-source and multi-temporal images requires the rectification of these images into the same geographic reference system.

Many software tools can be used to make geometric corrections as well as to rectify images (Toutin and Carbonneau, 1992). However, due to the physical characteristics of SAR

images such as the geometric distortion properties and speckle (Polidori, 1997), a difficulty remains; i.e., efficiently selecting ground control points (GCPs). Indeed, GCP selection is still today a manual operation. In addition, this process remains tedious because of the properties of SAR images—GCPs can be difficult to locate accurately due to speckle and layover—and to the inherent uncertainty in GCPs positions (e.g., if a road intersection has been moved a few meters but not updated on the topographic map). Moreover, in a few areas such as the far north and in deserts, the selection of GCPs is difficult to carry out because of the lack of easily identifiable features.

As in other countries (e.g., the United States with USGS topographic maps, China with NFGIS, New-Zealand with LAMPS2, Germany with ATKIS, or France with BDTopo), Geomatics Canada has developed a digital topographic database (TDB) covering the entire country: the National Topographic Database (NTDB, 2000). Moreover, from the NTDB, Geomatics Canada has built the Data Alignment Layer (CDAL), which "contains points that are easy to identify at different cartographic scales to allow the georeferencing of data from various sources" (Parent, 1999). The CDAL is part of the CGDI, i.e., the Canadian Geospatial Data Infrastructure (Labonte *et al.*, 1998). The method presented in this paper has been tested with Canada's NTDB and CDAL datasets to facilitate GCP selection in Radarsat images over Canada, but the concepts and approach can be adapted to other countries using their national topographic database and taking into account the particularities of their topography. For example, one may use the feature class "road intersections" (or a combination of several feature classes) instead of the sole feature class "lakes" if there are more of the former than of the latter (which is obviously not the case in Canada).

Several automatic registration methods have been developed over the past few years. These methods use techniques such as recognition of corresponding structures (Della Ventura *et al.*, 1990), feature matching (Dare *et al.*, 1997), features extracted from images or from digital databases (Dowman and Dare, 1999), correlation existing between two SAR images (CNES, 1996), or global image matching (Zhang *et al.*, 2000). However, these methods are not efficient with respect to every situation. For example, Iisaka and Sakurai-Amano (1996) developed an automated method for GCP selection, which uses

Centre de Recherche en Géomatique, Pavillon Casault, Université Laval, Québec, QC G1K 7P4, Canada.

B. Moulin and C. Djima are also with the Département Informatique, Pavillon Pouliot, Université Laval, Québec, QC G1K 7P4, Canada.

I. Couloigner is currently with the Department of Geomatics Engineering, University of Calgary, 2500 University Drive N.W., Calgary, AB T2N 1N4, Canada (couloigner@geomatics.ucalgary.ca).

Photogrammetric Engineering & Remote Sensing
Vol. 68, No. 5, May 2002, pp. 433–440.

0099-1112/02/6805-433\$3.00/0

© 2002 American Society for Photogrammetry
and Remote Sensing

road intersections and integrates information resulting from road maps. Although this method may prove useful in areas of high and medium density population, it cannot be used for several areas such as the Rockies, forested areas, and northern areas. One needs a generic approach that can be initiated differently depending upon the circumstances (type of topography, density of population, availability of map datasets, etc.).

We designed our approach with such issues in mind. We also targeted the potential users of our approach as being peoples with different levels of education (from students to trainees to professionals) and who work in various companies with different human, financial, and computer resources. These considerations led to designing two approaches: vector-based matching and raster-based matching. These two approaches require different resources and expertise to match candidate points or features extracted from Radarsat images with the corresponding points or features obtained from a topographic database. The matching process is applied to selected feature classes such as "water bodies" or "road intersections" (depending on the characteristics of the area) and allows the automated selection of a large number of potential GCPs, from which will be derived a subset including the "best" GCPs offering a good spatial distribution. Then the aim of the project is to create software that will enable the user to choose the type of topographic data (the NTDB versus the CDAL or other national TDB with some adaptation) he would prefer to use, the type of matching he should process to obtain a GCP list according to the skills he has in digital imaging of SAR imagery, the type of topographic data he could use and the commercial software that he could use, and finally the different types of features (one type only or a combination) from which he could extract the GCP list depending on what is available in the SAR image and in the topographic data of his area under consideration.

The next pages focus on the method used for the vector-based approach and the feature class "water body." This "vector-matching/water body" combination was justified by the specific context of our tests: two areas with numerous lakes and free availability of CDAL data. (Other tests were also made with the "raster-matching/water body" combination for research purposes). The method presented in this paper is divided into three steps: (1) extraction of water bodies from Radarsat images with their relevant information (center of mass, surface area), (2) extraction of the same type of information for lakes from the corresponding map sheets from the CDAL, and (3) matching the candidate points that will become GCPs—control points as well as check points of the rectification transformation—with the horizontal accuracy of the CDAL data.

Because the initial test area has areas of relatively gentle relief (700 to 1000 m of smooth elevation) with large water bodies (surface greater than 19,000 m²), the digital elevation information for the selected TDB points was not, at this time, integrated into the test procedure. Some recent work on the automatic registration of SAR geocoding using data derived from digital elevation models has been reported in the literature (e.g., Wegmueller, 1999). The geometric distortions inherent in SAR images have been taken into account in the recognition patterns used to match candidate GCPs.

Finally, Radarsat images of an area located east of Québec City is used as an example. This image corresponds to two map sheets of the NTDB at a scale of 1:50,000.

The Data

The study area is located around Québec City (QC, Canada). The site contains urban, agricultural, and forest zones. It includes the most typical GCPs, which are usually found in satellite images, such as road intersections and lakes.

The Radarsat data set is composed of three images in fine beam (F5) descending mode and one image in standard beam descending mode. The Radarsat data set includes Path Image

Plus products (pixel size: 3.125 m for the fine beam and 8 m for the standard beam) to enhance the ability to measure point targets. Image products are aligned parallel to the satellite's orbit path.

The NTDB data set is composed of four NTS (the National Topographic System of Canada based on the NAD83 datum) map sheets at a scale of 1:50,000 and one NTS map sheet at a scale of 1:250,000 for the Québec City area.

It is also important to know that the planimetric accuracy of the NTDB data can vary from one feature to another, but it is generally 10 m in urban areas, 25 m in rural areas, and 125 m in isolated areas. But this accuracy is a function of the type of data sources (BNDB, 1997).

This set is complemented with CDAL feature files corresponding to the NTS map sheets at a scale of 1:50,000. There are four CDAL feature files per NTS map sheet. These files are based on the points origin, i.e., intersection between roads/roads or roads/railways, point features, linear features, and polygon features (CDAL, 2000). Thus, CDAL feature files provide useful information for available objects, such as

- the center of mass of objects (e.g., for lakes and road intersections),
- the surface or the length of objects, and
- the number and the orientation of the road intersection branches.

The NTDB and CDAL provide data in geographic coordinates (latitude and longitude in decimal degrees), as is the case for Radarsat images. However, the Radarsat horizontal reference system seems to be based on the GRS75 ellipsoid, while the NTDB is based on the GRS80 ellipsoid.

The Developed Strategies

First of all, it is necessary to make a choice among the various features available in Radarsat images and in a topographic database such as the NTDB and CDAL. It is easy to filter a TDB by using SQL (Structured Query Language), because we know the feature category and the geographic coordinates of the area under consideration to which the features of interest belong.

However, according to the category of the objects under consideration and the approach used (vector-based or raster-based), image processing may be more or less easy.

Once the objects under consideration have been extracted from both images as well as from the topographic database, the two sources of data are matched for these points in order to identify GCPs (control and check points) with a well-known planimetric accuracy, for the category of interest. As we will see later, data matching can be done using a vector-based or a raster-based approach.

The next sections briefly describe how the categories of interest have been identified as well as the concepts used for the vector-based and the raster-based matching approaches.

Identification of the Features Common to the Radarsat Images and the TDB

Various types of features can be extracted from a TDB such as the NTDB or CDAL, in order to identify and characterize GCPs according to the possibilities of their detection and extraction from Radarsat images. These features are divided into three main categories:

- surface elements such as islands, water bodies (natural or artificial), and ski centers;
- point elements such as intersections between roads, roads and rivers, and highway exits; and
- linear elements such as road networks, rivers, bridges, and power line networks.

These three feature categories are easily extractable, using various database queries, from a TDB having proper feature/attribute coding. In the case of Radarsat images, the extraction of

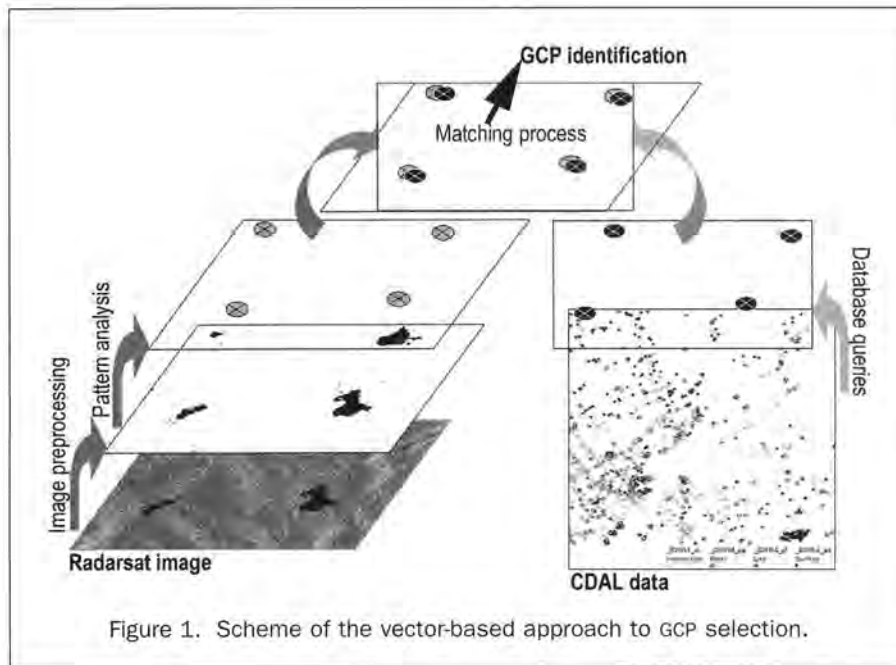


Figure 1. Scheme of the vector-based approach to GCP selection.

these feature categories is more or less easy and requires image processing.

Hence, the two data sources matching is carried out by feature category. The matching is divided into two major steps. First, the relevant information is related to the category "water body"; on the one hand, water bodies are easier to extract from satellite images and, on the other hand, water bodies, such as lakes, are very accurate for fixing GCPs. In a second step, the relevant information will be related to the category "intersection."

The Vector-Based Approach

The vector-based approach (Figure 1) consists in carrying out the two data sources matching in a vector database in order to select candidate GCPs and the control points for the transformation, i.e., the most accurate GCPs. For this purpose, vector-based recognition patterns are created using data extracted from Radarsat images. Other patterns are obtained using corresponding data from the CDAL. These recognition patterns are established from the centers of mass of the various extracted objects (see the next section). These recognition patterns allow us to take into account the geometric distortions in small relief areas due to SAR imagery acquisition in the two sets of data matching. The matching is based on the comparison of these recognition patterns, which provides the most accurate GCPs for the category of interest.

For this vector-based approach, only the CDAL data are necessary. The NTDB is only used to visually check the extracted features in a map form using GIS software. The CDAL files contain all the useful information in separate fields that are easily accessible using SQL. The files of interest are identified using the geographic coordinates of the area of study on the Radarsat image. One Radarsat area can include one or more NTS map sheets. The SQL queries are done file by file.

To obtain similar information (center of mass, surface, number of intersection branches, etc.) of the objects under consideration from Radarsat images, objects could be extracted from Radarsat images using commercial image processing software, and a pattern recognition algorithm has been developed to extract the useful information from the objects extracted according to the feature category to which the future GCP

belongs. These processes take into account the physical properties inherent in SAR images, such as the presence of speckle and relative geometric deformations.

This vector-based approach is presented in detail in the following sections for the category "water body." An application of this method in urban and forest areas is also shown.

The Raster-Based Approach

The raster-based approach (Figure 2) consists in matching selected features present in the NTDB files with their homologous features present in the SAR image in order to extract GCPs. First of all, matching regions, such as lakes, does the processing. Matching linear features, such as roads, will later complete it. The matching takes place in a raster environment. So, vector NTDB features are rasterized with commercial software. The rasterization allows each pixel to receive a single value. To improve the processing time, NTDB files (as well as the image) are divided into subscenes. An NTDB subscene, which includes several lakes, is subdivided again into mini-matrices. Each mini-matrix contains one lake. Some of the lake's geometric

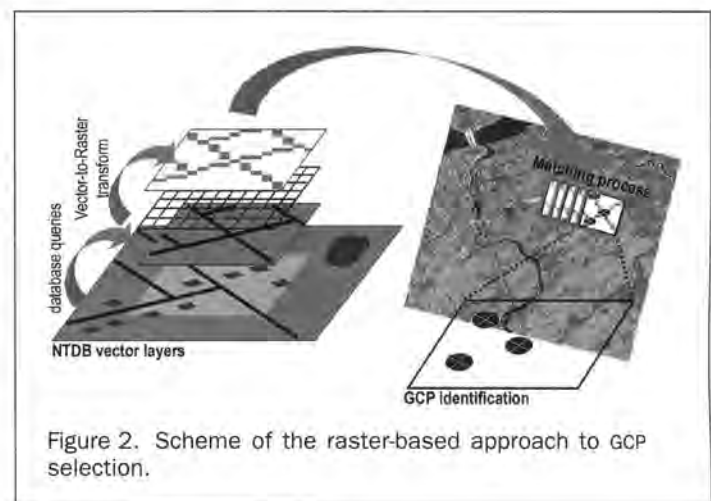


Figure 2. Scheme of the raster-based approach to GCP selection.

attributes (e.g., perimeter, area, and invariant moments) are also computed. These lakes are matched with their homologous lakes in the SAR image.

In this approach, the two sources of data matching are divided into two steps:

- a template matching where the sum of the corresponding gray level between a mini-matrix and the image is computed. High values are searched because they represent the regions where a good contrast exists between a low intensity region (possibly a lake) and its brighter gray level environment. High values are the starting point of a breadth-first search to extract the "lake." Some geometric attributes of the "lake" are also computed.
- a geometric comparison using a cost function is performed. This cost function is based on the difference between the geometric attributes of two corresponding lakes. A low value of the cost function implies a good match. GCPs are then extracted from the best match. For lakes, centers of mass represent good GCPs.

The raster-based approach relies on the fact that the user doesn't need to have a good knowledge of the image features. It tends to minimize the image processing (thresholding, image segmentation, etc.) generally done to extract some features in the image (cf. vector-based approach). A detailed account of the raster-based approach will be the subject of another paper.

Detailed Presentation of the Vector-Based Approach

At present, we have developed the approach by concentrating our efforts on GCP selection from the category "water body." The method to automatically identify this type of GCPs proceeds in four steps.

Extraction of Candidate GCPs from Radarsat Images

To extract water bodies from Radarsat images, different image processing tools can be used. In this case, a texture analysis algorithm was selected. This is because the two textures (water and forest areas) found in forest areas in Radarsat images are well discriminated. Moreover, in residential and urban areas, water texture is easily discriminated from the other textures present in the image. After testing different algorithms with different moving window sizes, the variance algorithm with a moving window size equal to 11 was selected to enhance Radarsat images texture. The resulting image presents a histogram with two well separated modes. To obtain the binary image of water bodies, a binary thresholding is then carried out on the bi-modal histogram. If there are rivers in the binary image, they are masked. Future users using commercial image processing software could easily perform this step.

Finally, we developed a pattern analysis algorithm that enables us to obtain the surface and the center of mass of the

extracted water bodies whose surface is greater than or equal to a given threshold. This algorithm is divided into two steps: find one first pixel belonging to a lake and then find all pixels belonging to the lake by a breadth-first search. This algorithm, which is integrated in the GCP software prototype, provides the image candidate GCPs for the area of study.

Extraction of Corresponding Candidate GCPs from CDAL Files

The extraction of the relevant information for water bodies is done file by file in the GCP software prototype using SQL. The criteria for queries depend on

- the geographical coordinates of the area of study on the Radarsat image. One Radarsat area may correspond to one or more CDAL files;
- the category of the feature under consideration: in this case, "lake";
- the attributes of interest for "lake": in this case latitude and longitude of centers of mass, and surfaces; and
- the constraint conditions: in this case, selection of all lakes whose surface is greater than or equal to a given threshold, e.g., equivalent to a surface of 2000 pixels.

These queries provide the CDAL candidate GCPs for the area of study.

Matching of the Two Sets of Candidate GCPs

There are now two lists of candidate GCPs with the same type of information obtained from the two data sources. To select good quality GCPs, i.e., with a well-known planimetric accuracy, these two lists are matched. This matching is divided into two steps:

- (1) connecting the centers of mass of extracted water bodies from images with the corresponding centers of mass of lakes obtained from the CDAL files; and
- (2) comparison of the recognition patterns established both for the image candidate GCP list and for the CDAL candidate GCP list. The recognition patterns are built with the (lake *l*, central lake) vectors, where the central lake is the lake located as the closest to the center of the area of study (see an example in Figure 6).

To enable the creation of (CDAL lake, image lake) pairs, several areas were examined in two Radarsat images of the Québec City area. The study has shown that the variations, measured for longitude and latitude, between the centers of mass of the CDAL lakes and the corresponding lakes extracted from images were relatively constant according to the NTS map sheet under consideration (see Table 1). Moreover, the planimetric accuracy of CDAL features depends on the NTS map sheet. Hence, the processes to select GCPs are performed map sheet by map sheet.

TABLE 1. VARIATIONS (IN DEGREE DECIMALS) IN LONGITUDE AND LATITUDE BETWEEN THE CENTERS OF MASS OF THE PAIRS (CDAL LAKE, IMAGE LAKE) INCLUDED IN TWO RADARSAT IMAGES IN FINE FAR BEAM FOR THE QUÉBEC CITY AREA

NTS map sheet	Image	Number of pairs	Δ latitude (in dd)		Δ longitude (in dd)	
			$\mu^{(1)}$	$\sigma^{(2)}$	$\mu^{(1)}$	$\sigma^{(2)}$
21M02	Zone 1 - Queb N	7	-0.0021	0.0002	0.0103	0.0008
	Zone 6 - Queb N	7	-0.0023	0.0004	0.0102	0.0008
	Total	14	-0.0022	0.0003	0.0103	0.0008
21M03	Zone 2 - Queb N	5	-0.0012	0.0002	0.0087	0.0005
	Zone 6 - Queb N	21	-0.0012	0.0002	0.0086	0.0007
	Zone 4 - Queb C	7	-0.0011	0.0002	0.0078	0.0006
	Zone 5 - Queb C	8	-0.0012	0.0002	0.0077	0.0006
	Total	41	-0.0012	0.0002	0.0083	0.0008
21L14	Zone 8 - Queb N	9	-0.0006	0.0003	0.0036	0.0020
	Zone 4 - Queb C	6	-0.0007	0.0001	0.0038	0.0004
	Zone 5 - Queb C	14	-0.0008	0.0002	0.0033	0.0012
	Total	29	-0.0007	0.0003	0.0035	0.0014

⁽¹⁾mean; ⁽²⁾standard deviation

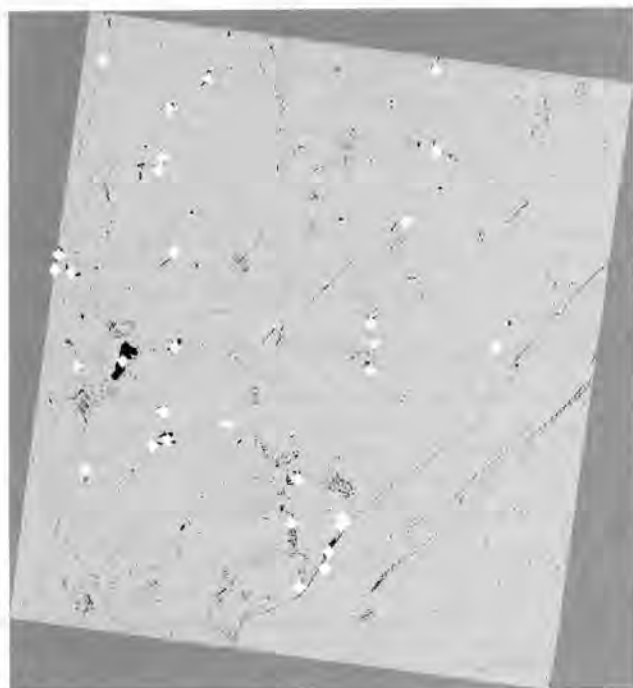


Figure 3. Water bodies extracted from the Radarsat image Lacs_cen. The white diamonds represent the center of gravity computed by the pattern algorithm from the binary image.

(CDAL lake, image lake) pairs are first created according to the following four steps:

- (1) a first list of paired lakes is obtained if $\text{longitude}[\text{image lake}] = \text{longitude}[\text{CDAL lake}]$ to the nearest one hundredth or if $\text{longitude}[\text{image lake}] = \text{longitude}[\text{CDAL lake}] + 0.01$;
- (2) a second list of paired lakes appears if $\text{latitude}[\text{image lake}] \leq \text{latitude}[\text{CDAL lake}]$ only for the first paired lakes;
- (3) among the CDAL lakes connected to one image lake, select the CDAL lake for which $(\text{latitude}[\text{image lake}] - \text{latitude}[\text{CDAL lake}])$ is maximum: a third list of paired lakes is obtained; and

- (4) for each third pair, if $(\text{latitude}[\text{image lake}] - \text{latitude}[\text{CDAL lake}]) \in [0.001; 0.0001]$, the pair is selected: the final list of the paired lakes is thus produced.

Second, the recognition patterns of paired lakes are built for the CDAL set and for the image set starting from their center of mass. The origin of these recognition patterns is the lake located the closest to the center of the study area. These recognition patterns enable us to take into account the geometric deformations in Radarsat images. Then, the (lake *l*, central lake) vectors norm and orientation relative to the cartographic North are computed (see an example in Figure 6). To compare the two recognition patterns, the differences in norm and orientation between two paired vectors are computed. To find the region of GCPs acceptance, the confidence intervals for the norm differences and for the orientation differences are then computed with a known degree of uncertainty. The user, according to his GCP needs, will choose this degree of uncertainty.

The GCP Selection

The selection of good quality GCPs, and of control points of the transformation function, is then made according to the following criterion:

if the norm and orientation differences of paired (lake *l*, central lake) vectors are included both in the norm and orientation confidence intervals, the pair for the lake *l* is selected as a good quality GCP.

The central lake is always considered as a GCP, because it is useful to have a control point located near the center of the image to be rectified.

GCP Identification from "Water Body": An Application

This section presents an application of our method to an area which represents the town of Beauport (East of Québec City), a part of the Orleans Island and the forest area located north of Québec City. The image selected for this area of interest was issued from the F5F fine Radarsat scene centered on 46°49' N; 71°01' W, acquired in July 1997 and called Lacs_cen. Its size is 8750 lines by 7783 columns, which represents one quarter (25 by 25 km) of the Radarsat scene.

Figure 3 presents a binary image of water bodies, as well as their center of mass (represented by a white diamond), that

E: Liste des GCP CCDI				
Fauille	Geometrie	Superficie	Latitude	Longitude
21L14	POLYGOONE	18075	46.92086	-71.2067
21L14	POLYGOONE	36760	46.87042	-71.1558
21L14	POLYGOONE	162839	46.87745	-71.1532
21L14	POLYGOONE	59375	46.86949	-71.1294
21L14	POLYGOONE	17902	46.96127	-71.1281
21L14	POLYGOONE	18927	46.98558	-71.1059
21L14	POLYGOONE	35543	46.95896	-71.0564
21L14	POLYGOONE	24366	46.86679	-71.0475
21M03	POLYGOONE	49771	47.08567	-71.3013
21M03	POLYGOONE	23213	47.08985	-71.2851
21M03	POLYGOONE	23083	47.02827	-71.2675
21M03	POLYGOONE	44930	47.03247	-71.2673
21M03	POLYGOONE	31480	47.03124	-71.2583

(a)

E: Liste des GCP Image			
Fauille	Superficie	Longitude	Latitude
21L14	20250	-71.1517	46.8765
21L14	2449	-71.2374	46.8959
21L14	3680	-71.1544	46.8698
21L14	2045	-71.1583	46.8687
21L14	3128	-71.1230	46.8626
21L14	2230	-71.1257	46.8603
21L14	2647	-71.1889	46.8618
21M03	2001	-71.2078	47.0836
21M03	2220	-71.2779	47.0889
21M03	2689	-71.0890	47.0690
21M03	12585	-71.2200	47.0664
21M03	2513	-71.2816	47.0738

(b)

Figure 4. CDAL list of GCP candidates (a) and Image list of GCP candidates (b) computed by the GCP software for a lake surface greater than or equal to 1800 pixels (equivalent to 17,578 m²).

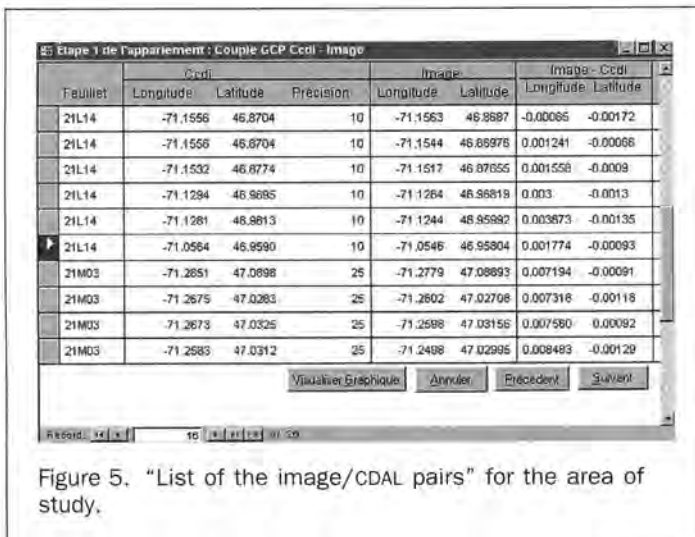


Figure 5. "List of the image/CDAL pairs" for the area of study.

are extracted from Lacs_cen using texture analysis and a manual binary thresholding. Many lakes appear in this image. This image is one of the inputs to the GCP software prototype.

For the application, the study area only includes two NTS map sheets at a scale of 1:50,000 : 21L14 and 21M03. The "21L14_ps" and the "21M03_ps" files have been free-downloaded from the CDAL website (CDAL, 2000).

After entering these inputs in the GCP software prototype, it enables the CDAL candidate GCPs identification which are displayed on the following screen (Figure 4a) and the computation of the water bodies center of mass and surface (Figure 4b). Thirty-seven CDAL lakes—23 in the 21L14 map sheet and 14 in the 21M03 map sheet—with a horizontal precision of 10 m and 25 m, respectively, and 46 water bodies—32 in the 21L14 map sheet and 14 in the 21M03 map sheet—correspond to Figure 3. It took 47.18 seconds, in CPU time, to obtain these lists with an AMD-K6 processor with 128MB of RAM; hence, the GCP software

significantly decreases the time used by an operator to manually select GCPs in a satellite image.

After these first steps, the prototype enables the matching process that displays the pairs of image/CDAL lakes (Figure 5). In our application, there are 26 (CDAL lake, image lake) pairs—16 in the 21L14 map sheet and ten in the 21M03 map sheet. It also allows the user, if he wants, to see the recognition patterns of all candidate image/CDAL GCP (Figure 6). As we can see in Figure 6, the deviation between the two recognition patterns seems to be more important for the 21M03 map sheet (above 47°N) than for the 21L14 map sheet (below 47°N). Moreover, this figure shows that the geometric deformation due to the SAR acquisition principle is weak.

After the selection of the degree of uncertainty (e.g., 0.05) that the user wants for the GCP acceptance area, the prototype enables the process which will select the most accurate GCP, i.e., the control points for the transformation, based on the chosen degree of uncertainty. A report on the matching process could be displayed and printed. Then, the user may choose to select another degree of uncertainty, and repeat the process if he is not satisfied.

Finally, there are two choices for the user:

- (1) If there is a new area to process, the user can repeats all the steps to have GCPs for this area of study.
- (2) If he has processed all areas of study of the Radarsat scene, the final GCP list is displayed (Figure 7). In our case, 13 GCPs have been selected for the 0.02 degree of uncertainty.

A user can choose the final GCPs according both to the number and to the horizontal accuracy of GCPs that he wants. With our software, a user will also be able to display a figure (such as Figure 8) to locate the selected GCPs in the study area. In this way, a user can see if the selected GCPs are well distributed in the image or if he will need other GCPs. Thus, in our case, only the right quarter of the area of study has GCPs. This result is normal, because there are few lakes in the other parts of Figure 3.

Hence, a user has to choose another degree of uncertainty or another category, such as "road intersection," to obtain more

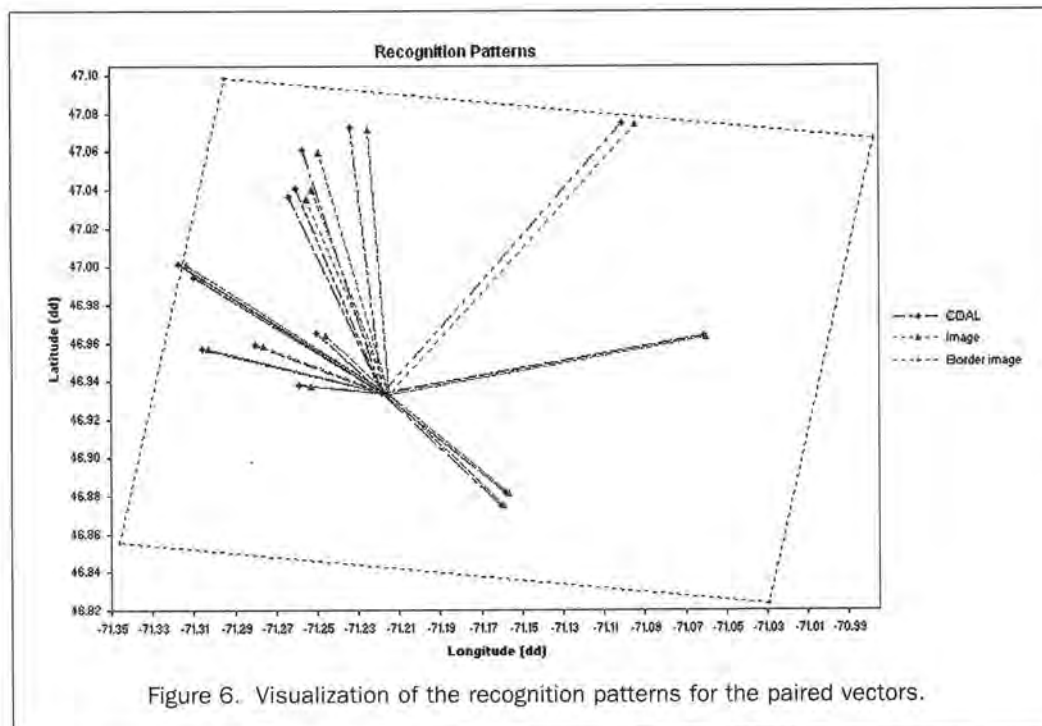


Figure 6. Visualization of the recognition patterns for the paired vectors.

Fichier	Circi			Image			Nom	N.C.
	Longitude	Latitude	Préc.	Longitude	Latitude			
21L14	-71.3046	46.9997	10	-71.3007	46.98897	E\lacs2_cen.raw		0.98
21L14	-71.3070	46.9616	10	-71.3035	46.96098	E\lacs2_cen.raw		0.98
21L14	-71.3122	46.9965	10	-71.3080	46.99585	E\lacs2_cen.raw		0.98
21L14	-71.3147	46.9906	10	-71.3106	46.98998	E\lacs2_cen.raw		0.98
21M03	-71.2516	47.0557	25	-71.2437	47.05454	E\lacs2_cen.raw		0.98
21M03	-71.2548	47.0359	25	-71.2472	47.03508	E\lacs2_cen.raw		0.98
21M03	-71.2673	47.0325	25	-71.2590	47.03156	E\lacs2_cen.raw		0.98
21M03	-71.2675	47.0283	25	-71.2602	47.02708	E\lacs2_cen.raw		0.98
21M03	-71.2851	47.0886	25	-71.2779	47.08893	E\lacs2_cen.raw		0.98

Figure 7. Final GCP list for the study area.

GCPs for this image in order to merge it with other images or to georeference it.

The software prototype that we developed will assist the user by applying the method step by step, which makes it easy for users who are not specialists in remotely sensed image rectification.

Application of the Selected GCPs to Rectify a Radarsat Image

Different applications have been tried out using the GCP software prototype. The selected GCPs for Lacs_cen were used to reference the image to the NTDB horizontal reference. The GCP software was also used to find the GCPs of the Lacs_north Radarsat image needed to reference it to the NTDB horizontal reference. The Lacs_north Radarsat image was obtained from the fine F5F Radarsat scene centered on (46°35'N; 71°35'W) and acquired in August 1997. This image represents the same area of interest as the Lacs_cen. The GCP software enabled the selection of 16 GCPs with ten control points at a 0.02 degree of uncertainty.

For the image's referencing, the second-order polynomial transformation was used with the selected GCPs as control points. Once both images were rectified, the fusion of the two

images has been processed. Figure 9a shows the fused image: Lacs_cen is in the blue channel and Lacs_nord in the red and green channels. The zoom provided in Figure 9b shows that there is no geometric displacement between the two images. With the fusion of these images, the tidal effect on the St Laurent River is visible both on the Orleans island and on the Beauport coastal zones.

Conclusion and Perspectives

The aim of our project is to develop methods and software tools to automatically identify GCPs with a known horizontal accuracy in Radarsat images using a topographic database such as the national topographic database of Canada. These GCPs will be used to carry out several tasks, such as geometrical corrections of images and multi-source image registration. Various strategies are proposed to achieve these objectives so that the user will be able to choose the appropriate strategy according to the characteristics of the land surface, to the period of the year, and to the resources that are available in his organization. These strategies are elaborated according to two matching approaches of the two data sources: the vector- and raster-based approaches. Because the image processing is a disjoint step of the developed strategies, they can be applied to other satellite data.

A vector-based method was developed to automatically identify GCPs—control and check points—in Radarsat images for the elements belonging to the category “water body.” The GCPs elevation information was not integrated at this time due to the smooth elevation of the areas of interest. The method gives good results according to the degree of uncertainty of the selection tests. The user can define the desired degree of uncertainty. The final choice of GCPs depends on the user's choice of number of GCPs and of the GCPs horizontal accuracy that is needed. The vector-based approach has been presented in this paper.

For the vector-based approach, the development of a method to identify good quality GCPs that belong to the category “road intersection” is in progress; it will be used jointly with the category “water body” and may prove to be very complementary. In parallel, a study is currently being carried out to find a method for the raster-based approach, which may also be used in a stand-alone manner or jointly with the vector-based methods. For this project, future works will integrate the elevation

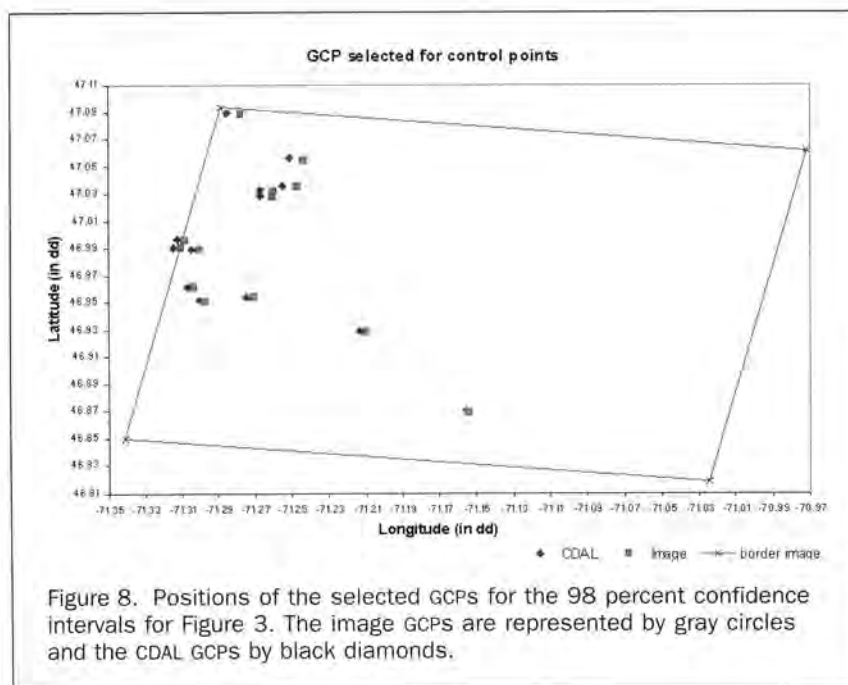


Figure 8. Positions of the selected GCPs for the 98 percent confidence intervals for Figure 3. The image GCPs are represented by gray circles and the CDAL GCPs by black diamonds.

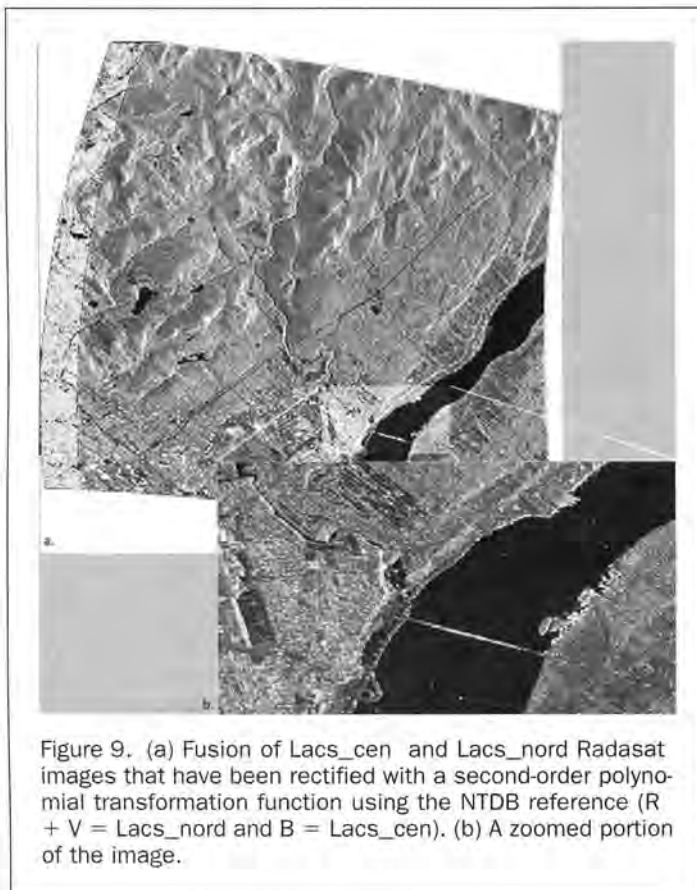


Figure 9. (a) Fusion of Lacs_cen and Lacs_nord Radarsat images that have been rectified with a second-order polynomial transformation function using the NTDB reference ($R + V = \text{Lacs_nord}$ and $B = \text{Lacs_cen}$). (b) A zoomed portion of the image.

information of selected GCPs in order to provide geometrically corrected images with good horizontal and vertical precision and also to automate orthorectification.

Finally, the availability of such automated GCP selection software will allow people to use topographic databases or alignment layers (where available) to automatically apply geometric corrections to Radarsat images as well as to other satellite images, and to improve the cartographic accuracy of the rectified images. Thus, it will be easier to integrate the rectified images into spatially referenced databases. Moreover, GCPs superabundance will ensure a better spatial distribution of these points and, consequently, a higher cartographic accuracy for the users of Radarsat images.

Acknowledgments

The authors wish to acknowledge the financial support of the Quebec FCAR Funds' Action Concertée Program in collaboration with Radarsat International, the latter also providing the

images. We also thank Geomatics Canada, both at the Centre for Topographic Information in Sherbrooke who gave the NTDB files and answered our many questions, as well as the Canada Centre for Remote Sensing in Ottawa, especially Dr. Thierry Toutin, for their precious advices.

References

- BNDT, 1997. *Normes et spécifications de la base nationale de données topographiques, édition 3.1*, Technical Manual of Geomatics Canada, Sherbrooke, QC, Canada, 32 p.
- CDAL, 2000. Official website of the CGDI (Canadian Geospatial Data Infrastructure) Data Alignment Layer designed, operated and maintained the Centre for Topographic Information in Sherbrooke, QC, Canada, URL: <http://www.cits.rncan.gc.ca/~cdal/>.
- CNES, 1996. *Philosophy and Instructions for the Use of the DIAPASON Interferometry Software System Developed at CNES*, Technical Manual of the French Spatial Agency, Toulouse, France.
- Dare, P.M., R. Ruskoné, and I.J. Dowman, 1997. Algorithm development for the automatic registration of satellite images, *Proceedings of IRW '97*, 20–21 November, NASA Goddard Space Flight Center, Greenbelt, Maryland, 10 p.
- Della Ventura, A., A. Rampini, and R. Schattini, 1990. Image registration by recognition of corresponding structures, *IEEE Transactions on Geoscience and Remote-Sensing*, 28(3):303.
- Dowman, I.J., and P.M. Dare, 1999. Automated procedures for multi sensor registration and orthorectification of satellite images, *Proceedings of the International Archives of Photogrammetry and Remote Sensing*, 03–04 June, Valladolid, Spain, 32(Part 7-4-3 W6):37–44.
- Iisaka, J., and T. Sakurai-Amano, 1996. Automated GCP detection for SAR imagery: I. Road intersections, *Proceedings of the International SPIE Symposium on Optical Science, Engineering and Instrumentation*, 04–8 August, Denver, Colorado, 5 p.
- Labonte, J., M. Corey, and T. Evangelatos, 1998. CGDI-geospatial information for the knowledge economy, *Geomatica*, 52(2):194–200.
- NTDB, 2000. Official website of the National Topographic DataBase designed, operated, and maintained by the Centre for Topographic Information in Sherbrooke, Canada, URL: <http://www.ccg.rncan.gc.ca/ext/html/english/products/ntdb/ntdb.html>.
- Parent, Ch., 1999. The CGDI data alignment layer, *Geomatica*, 53(3):326–330.
- Polidori, L., 1997. *Cartographic Radar*, Gordon and Breach Science Publishers, Amsterdam, The Netherlands, pp. 35–60.
- Toutin, T., and Y. Carbonneau, 1992. MOS and SEASAT image geometric corrections, *IEEE Transactions on Geoscience and Remote Sensing*, 30(3):603–609.
- Wegmueller, U., 1999. Automatic terrain corrected SAR geocoding, *Proceeding of IGARRS'99*, 28 June–02 July, Hamburg, Germany, pp. 1712–1717.
- Zhang, Z., J. Zhang, M. Liao, and L. Zhang, 2000. Automatic registration of multi-source imagery based on global image matching, *Photogrammetric Engineering & Remote Sensing*, 66(5):625–629.

(Received 22 September 2000; accepted 03 July 2001; revised 17 August 2001)